



Study of defects and dimensional accuracy to determine manufacturability thresholds for laser powder bed fusion of Ti-6Al-4V lattices

Mohammad Reza Vaziri Sereshk¹ · Eric Faierson¹

Received: 2 August 2022 / Accepted: 12 October 2022 / Published online: 20 October 2022
© The Author(s), under exclusive licence to Springer-Verlag London Ltd., part of Springer Nature 2022

Abstract

The degree to which lattice structure fabricated by additive manufacturing (AM) processes matches the original solid model depends on a number of factors, some of which include type of AM process, machine characteristics, and powder utilized. Although some thresholds on dimensions or orientation for 3D-printed simple bars or plates are available in the literature, a large number of variables that influence lattice 3D-printing require thorough investigation. In particular, numerous build orientation for inclined struts, heat dissipation in complex geometry, and structural joints are some unique features of lattices which should be considered while developing associated thresholds. Experimental observation indicated different sizes for similar struts at different locations on a lattice. This requires investigation on the influence of build orientation. In this study, a wide range of strut- and surface-based lattices were designed and fabricated from Ti-6Al-4V in order to study defects and dimensional accuracy. Manufacturability limitations and design considerations were evaluated to achieve a product that was representative of the original design in terms of both geometry and dimensional accuracy. It is demonstrated that below the identified thresholds, the orientation of the lattices on the build-plate influences the homogeneity and dimensional accuracy. Acceptable homogeneity in geometry was achieved for entire lattice structure after orienting 45° around two Cartesian axes. It is demonstrated that support structure should be enough large to facilitate heat dissipation and reduce thermal distortion.

Keywords Manufacturability thresholds · Lattice · Dimensional accuracy · Defect · Build orientation

1 Introduction

Additive manufacturing has enabled designers to develop parts with complex geometries such as lattice structures. Considering the nature of layer-wised fabrication techniques, as well as some technology limitations including laser spot size and powder particle size, fabricating delicate parts at required dimensions and without implementation of structural support is still a challenge to fully realize the advantages of lattice structures.

Tang et al. [1] discussed some of the challenges for laser powder bed fusion (LPBF) method. These include optimum scanning pattern, permissible overhang and bridge length, minimum angle of inclination, and cantilever area of slanted

struts. Some effects are inherent to AM process. The staircase effect due to the accumulation of adhered powder on upskin and downskin surfaces is explained by Cabanettes et al. [2]. Surface roughness is another inherent feature of LPBF process. Its negative effect on the porosity of lattices is discussed in Alghamdi et al. [3] and Chahid et al. [4]. Approaches like electrochemical machining is suggested to mitigate undesirable surface roughness [5, 6]. EBSD analysis can provide inverse pole figures to study microstructural changes from powder to struts at different inclination angles [7]. Gangireddy et al. [8, 9] discussed grain boundary alteration during solidification and after post-processing operations.

Some other features of AM processes may lead to defects or dimensional error. Curved strut is a defect observed by Harris et al. [10] on the SEM micrographs. Yan et al. [11] discussed powder particle size and shape. They examined SEM and micro-CT scan images to identify partially melted powder particles that bonded to the boundary of solidified layers and discussed how this phenomenon influences the

✉ Mohammad Reza Vaziri Sereshk
mrvaziri2000@yahoo.com

¹ Quad City Manufacturing Lab-Western Illinois University,
Rock Island, IL 61201, USA

dimensions of struts. Similar observations were reported in Al-Saedi et al. [12]. Dimensional accuracy is a concern which was examined by Scalzo et al. [13] for struts at different inclination angles. However, the possibility of formation of flaws increases if the struts are designed to be printed with diameter below certain limit [14]. Therefore, identifying AM thresholds is a crucial design step for lattices.

Several approaches are presented in the literature to identify manufacturability thresholds for LPBF process. Calignano [15] designed some samples with overhanging structures (thin walls) to discuss the limitations for printing structures with a downward sloping face. Similar approaches were used to determine general limitations by researchers in Su et al. [16] and Wang et al. [17]. However, Mazur et al. [18] proposed an approach more relevant to lattices by manufacturing cantilever rods test block specimens. These test blocks consisted several circular bars for a range of inclination angles and rod sizes to determine the manufacturability thresholds based on the existence of flaws. However, lattices consist either several struts at different inclination angles or shells with sophisticated 3D curvature. They hold unique features that may require particular attention. For example, adjusting real angle of orientation for all struts in specific range would not be possible in some cases (e.g., Octet-Truss) even by rotating the sample on the build-plate, or size of short struts may change adjacent to structural joints. In addition, heat accumulation and dissipation are different when printing a lattice with many adjacent struts, as compared to printing a single bar. Although general thresholds for printing unit-cell components, including thin walls or delicate struts, may be applicable for design of lattices, the effects of noted unique features would be missed. In this study, a set of several strut- and surface-based lattices were printed from Ti-6Al-4V. They were examined not only for the visible flaws, but also for dimensional errors to determine corresponding manufacturability thresholds. It was observed that similar struts at different locations on a lattice were printed at different sizes. Therefore, the influence of build orientation was investigated, as well.

2 Lattice samples

The limits of the additive manufacturing process need to be considered in regard to strut/wall dimension and orientation to eliminate the need for support structure. Samples with Diagonal, Diamond (also known as body-centered cubic (BCC) or octahedral), FCC, and Gyroid unit cells were chosen as representatives of strut- and surface-based lattices. They were printed from Ti-6Al-4V powder at different sizes and orientations with an EOS M270 machine based on the process parameters recommended by EOS. Table 1 summarizes the dimensions of struts, cell sizes, and lattice samples. All dimensions are in mm.

3 Flaws

The first set of lattices was printed on one edge after 45° rotation. Figure 1a shows 3D model of the oriented sample on build-plate by rotation around Y-axis. The center of the sample was the center of rotation. Materialise Magics was used for build file preparation.

Figure 2a, b shows some of the observed flaws for samples #2 and #5 (marked as 22 and 3 on samples). The structural support was not removed to indicate the build orientation of the samples shown.

Figure 2a, b show flaws in the printed samples including missing or partially printed struts replaced by yellow lines. These defects were mainly observed for inclined struts. The cause is the change in strut angle after orientation on build-plate. Figure 3 demonstrates this phenomenon schematically for an inclined strut located in back side/plane of the sample. The apparent angle of strut with X axis is 45°. However, the real angle of orientation with build-plate would be 33° after 45° rotation of sample around the X-axis. This dangerously low angle for build orientation causes flaw when printing without support material.

Table 1 Dimension of the samples for manufacturability study

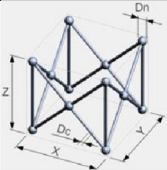
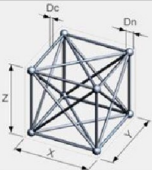
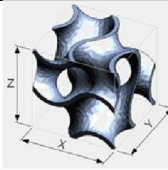
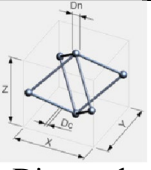
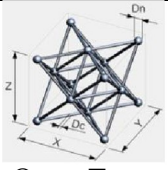
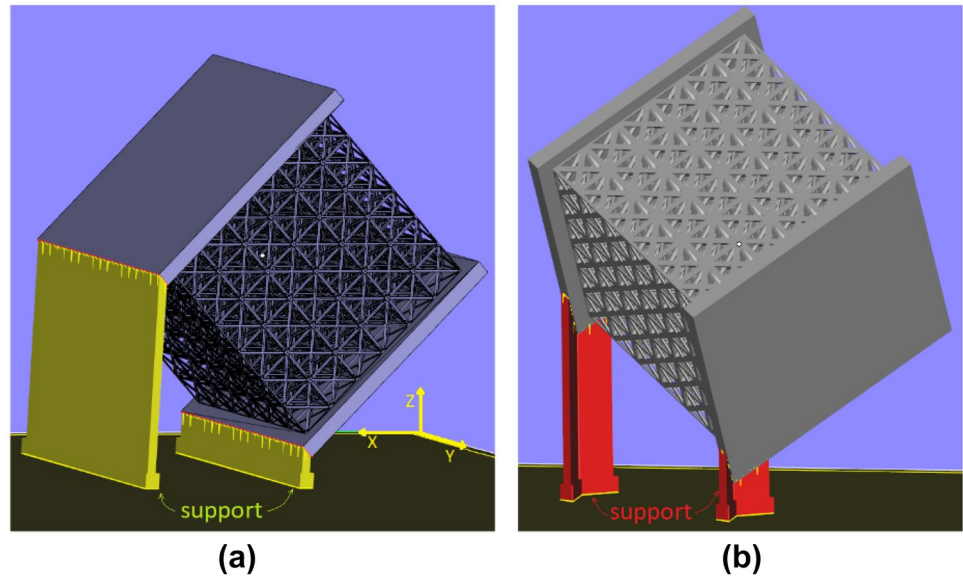
Sample #	1	2	3	4	5	6	7	8	9	10	11	12	13
Cell type	 Diagonals			 FCC			 Gyroid			 Diamond	 Octet-Truss		
Cell size	1.67	2.5	2.5	1.67	2.5	2.5	1.67	2.5	2.5	1.67	2.5	2.5	5
Strut diameter	0.2	0.2	0.4	0.2	0.2	0.4	0.1	0.1	0.3	0.2	0.4	0.6	0.4
Sample size	10	15	15	10	15	15	10	15	15	10	15	15	30

Fig. 1 Orientation of sample, **a** on edge, **b** on corner



The severity of flaws shown in Fig. 2 varies for different sides of the sample in terms of the number and distribution. This is due to the fact that rotating the sample around only one axis changes the real angle of orientation for similar struts unevenly. To get the maximum benefit out of the manufacturability thresholds, the samples were rotated 45° around the second axis (X) in the horizontal plane and the samples were printed on one corner (see Fig. 1b). This approach for orientation guarantees uniformity in geometry at similar planes. Figure 4 indicates different views of diagonals samples #3, #2, and #1 as well as FCC samples #6, #5, and #4 in left to right arrangement (see Table 1 for dimension). It is indicated that flaws exist for strut diameter of 0.2 mm, even for shorter strut span of 1.67 mm (samples #1 and #4). Since no flaws (missing or partially printed struts) were observed on samples #3 and #6, it can be concluded

that the struts with the minimum diameters of 0.4 mm can be manufactured without printability issues (flaws). However, they are examined for dimensional accuracy in Sect. 5.2.

The self-supporting properties for curved walls resulted in fabrication of all sizes of Gyroid lattice samples without any visible flaws at all sides. Samples #7 to #9 are evaluated in terms of dimensional accuracy in Sect. 5.3.

4 Defects

Lack of fusion defects was often observed on horizontal struts located at the top and bottom sides. These struts which remain horizontal after orientation need to be printed as a long, thin rectangle across each layer. This increases the possibility of defect formation compared to inclined struts with elliptical cross section at each layer. Figure 5 shows two defects indicated with red arrows.

It was observed that a few struts (identified by red arrows in Fig. 6) were not printed straight. For the struts inclined at very low angles at the top and bottom sides of lattices, a relatively large cross-section is printed on the top of powder. Depending on the rigidity of surrounding powder, the momentum of laser shots, or interaction with recoating wiper, the struts may deviate from the nominal CAD design.

5 Dimensional accuracy

5.1 Geometry mapping

Sample #10 (diamond lattice) is evaluated for feasibility and quality of printing of inclined struts over short span lengths. Figure 7 compares CAD geometry (red lines) with

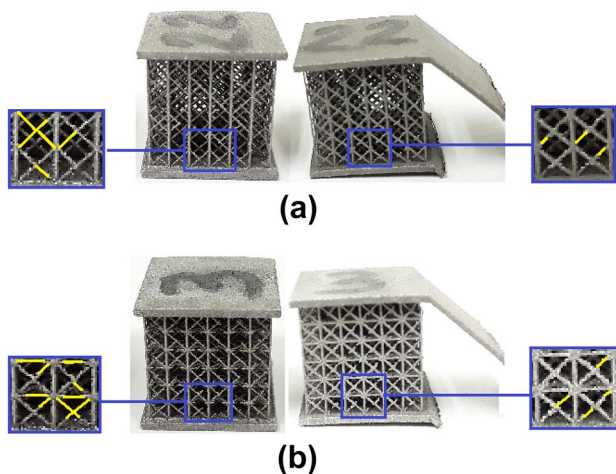
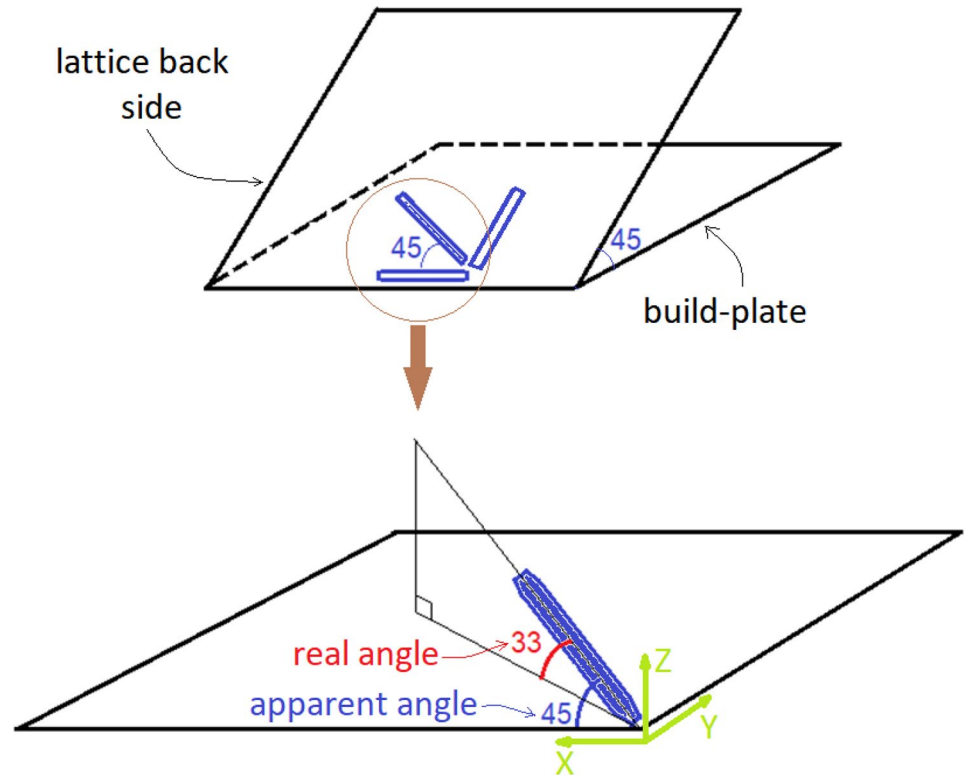


Fig. 2 Additively manufactured lattice samples; **a** flaws for sample #2, **b** flaws for sample#5

Fig. 3 Apparent angle in lattice side plane and real angle with build-plate after orientation



scanning electron microscopy (SEM) image of struts at different angles.

Some flaws are observed at the strut joints in Fig. 7. Larger nodes should be used to improve the design. It was demonstrated in Fig. 7 that lattice struts can be manufactured at any angle without structural support if the strut length is cautiously small, but the strut diameter was noticeably oversized. The larger than nominal strut diameters leads to reduction in the expected cell porosity which affects volume fraction. It changes the onset of full densification for lattice under compression, as well. Therefore, it is an important defect which influences the property of lattices significantly. The phenomena affecting dimensional accuracy is discussed next.

5.1.1 Partially melted powder particles

The larger diameters of the printed struts when compared to nominal CAD design (see Fig. 7) is a result of both powder particle size distribution (15–45 μm) and the small difference between nominal strut diameter (200 μm) and the laser spot size of $\sim 100 \mu\text{m}$. Figure 8a indicates the scanning process relevant to printing of a strut if it is viewed perpendicular to build direction. Green and purple bands are two adjacent laser tracks acquired for printing 200- μm struts having 100- μm laser spot size. As shown in Fig. 8a, some particles with the average size of 40 μm are partially melted on the boundary. This phenomenon can impact dimensional accuracy considerably if powder

Fig. 4 Flaws at top side (top) and left side (bottom); **a** diagonals samples, **b** FCC samples

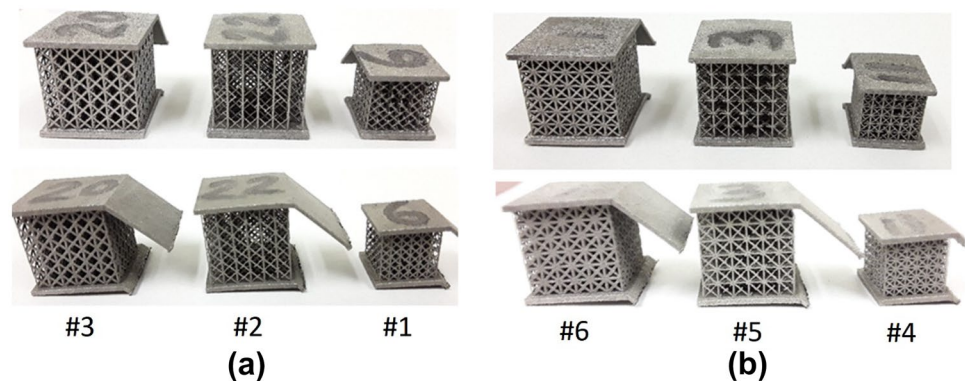
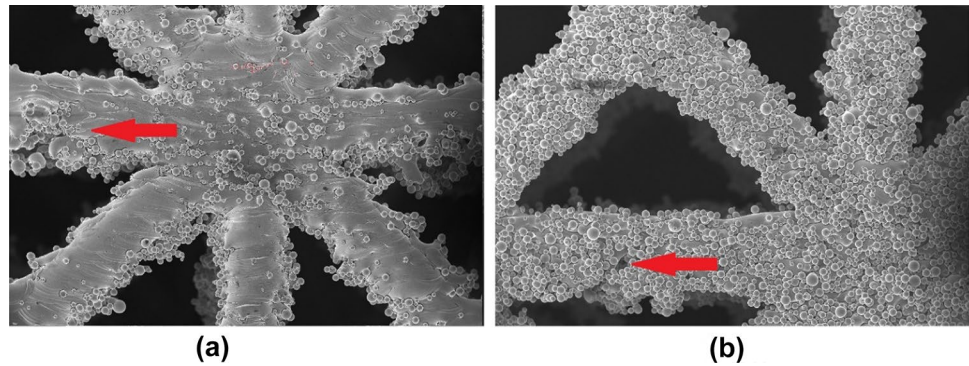


Fig. 5 Lack of fusion defect on struts; **a** top side, **b** bottom side



particle size is comparable with strut dimension [11]. Some of partially melted particles are indicated in SEM image of Fig. 8b by red arrows. Melt pools boundary can be seen as concave lines oriented perpendicular to build direction.

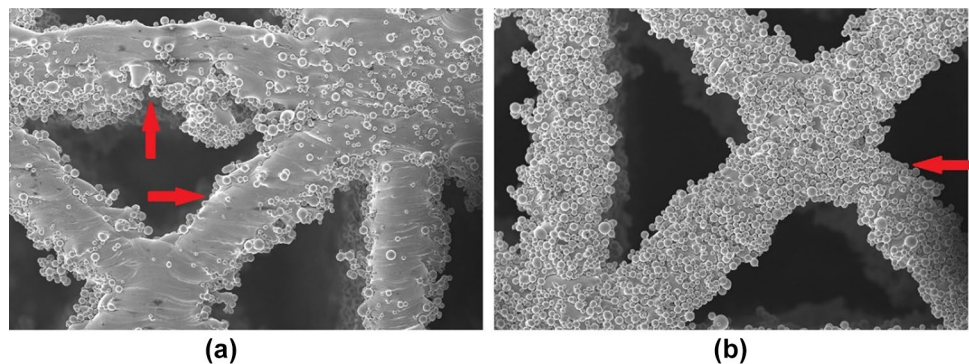
5.1.2 Staircase effect

The SEM image in Fig. 9 shows another phenomenon affecting dimensional accuracy. It is high level of powder adhesion underside inclined struts which are subject to staircase effect. Additional powder is captured by the melt pool (boundary indicated in schematic at Fig. 9) during layer formation which generates a rough surface for the underside of objects relative to build orientation.

5.1.3 Rough bottom for horizontal struts

Due to superior thermal conductivity of the solid lattice struts if compared to adjacent powder, the heat dissipates very fast and reduces melt pool temperature considerably by the time when wiper expands the powder for the next layer. This phenomenon prohibits adhering powder particles of the next layer to top of already melted layer. This generates considerably smoother surface at the topside of object. This effect is clearly revealed in Fig. 10, comparing top-side and bottom-side of FCC lattice sample.

Fig. 6 Curvature on the struts; **a** top side, **b** bottom side



5.2 Planar dimensional accuracy of struts

The orientation of lattices with respect to the build-plate changes the real angles for struts during the printing process (see Fig. 3). Therefore, struts with identical apparent angles located on different side planes are actually printed with different angles, which can disrupt the nominal homogeneity of the lattice structure geometry. To investigate the significance of this variation, as-built FCC sample #6 (without any visible flaw) with nominal strut diameter of 400 μm is considered. SEM images were prepared for struts at different locations for each side plane. ImageJ software was used to measure diameters at several longitudinal locations (at least 20 locations) along the struts. Figure 11 shows strut diameter measurements at apparent angles of 0, 45, 90, and 135° located at different side planes of top, bottom, left, and right.

Measurements in Fig. 11 indicated that all struts were printed oversized. Each box and whisker chart created by Excel software shows distribution of data into quartiles, highlighting the mean as well as the colorful box indicating one standard deviation above or below the mean. In general, the maximum average diameter (mean value) was below 500 μm and with maximum of 25% deviation from CAD geometry. Figure 11a demonstrates that the maximum deviation (mean) and larger range of variation (standard deviation) occurs for struts with apparent angle of zero, which are

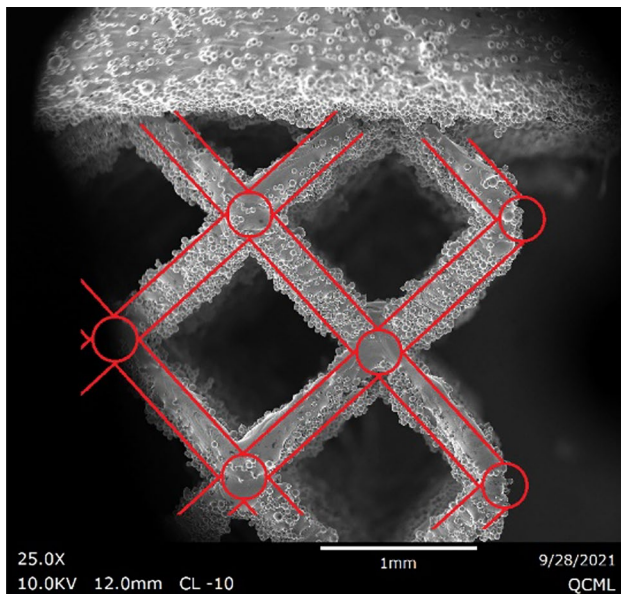


Fig. 7 CAD geometry (red lines) and SEM image of struts for diamond sample #10

printed on the bed of powder. Since, there was a symmetry in design and fabrication aspects for struts at right and left sides, average diameters differ slightly. This minor deviation may be due to difference in laser scanning pattern and difference in heat exchange with neighboring lattices.

5.3 Dimensional accuracy of shells

Thin walls in surface-based lattices provide a larger pathway for heat dissipation. Therefore, they were expected to have a more predictable melt pool size and consequently more accurate dimensions compared to strut-based lattices. Samples #7 to 9 are examined using SEM for images and ImageJ software for measurements. Figure 12 is a sample of SEM images and Fig. 13 summarizes the measurement.

Figure 13 indicates that Gyroid lattice walls were printed oversized in thickness. The deviation from CAD

geometry was higher for lower thicknesses. In fact, walls with nominal thicknesses of 100 μm were printed double-sized. In the case of very thin shell thickness of 100 μm , the melt pool is larger than laser spot (about 100 μm) [10]. Because the residual heat from previous and adjacent laser pulses increases, the accumulated heat and thinner walls are poorer pathway for heat dissipation. In addition, laser beam scans the contours that are made around the perimeter as part of the exposure process. However, more accurate dimensions for thicker Gyroids are due to larger heat pathway (thicker walls) leading to smaller (relative to strut) and more accurately predicted and adjustable melt pools. As a conclusion, although any visible flaw is not observed on thin walls of surface-based lattices for thicknesses as small as 100 μm , the dimensional error is significant and the geometry does not follow CAD design. Therefore, the threshold of 0.3 mm is recommended as the minimum thickness of thin walls.

6 Effect of build orientation

As it is indicated in Fig. 2a, b, flaws were not distributed evenly on different sides of the lattice printed on one edge. To achieve symmetric geometry, samples #2 and 5 were rotated 45° around two axes (X and Y) and printed on one corner as the one shown in Fig. 1d. Since the strut size below the determined threshold of 0.4 mm, significant number of flaws exist on different sides of the printed lattices shown in Fig. 14. However, distribution of flaws is uniform in terms of size and severity among different sides. SEM images in Fig. 15 show details of the printed struts with dimensions below the identified thresholds, and provide a clearer understanding of some of the defects difficult to detect with the naked eye. Significant variation in strut size along the length was observed. This variation is different for struts inclined at different angles. This was not observed for the struts printed at the sizes above the thresholds. Therefore, dimensional accuracy is more sensitive to orientation for the sizes below the thresholds.

Fig. 8 Partially melted powder particles at the layer boundary, **a** schematics (viewed perpendicular to build direction), **b** red arrow in SEM image (top side with $\times 361$ magnification)

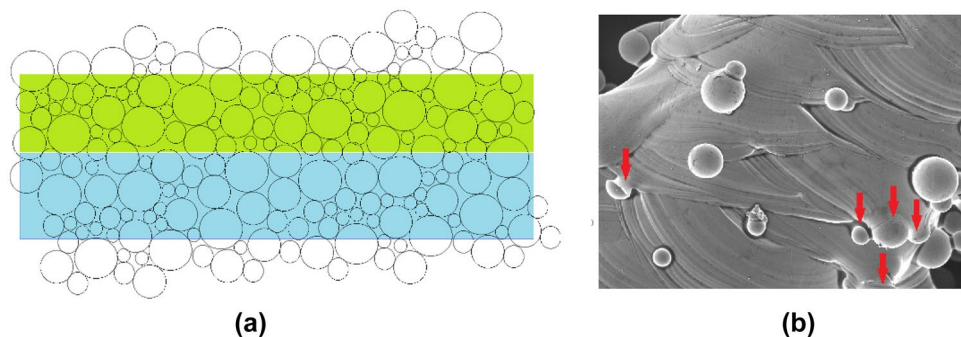
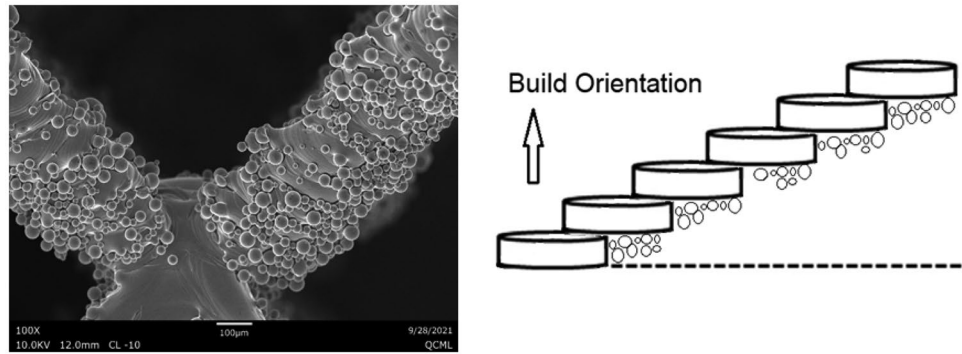


Fig. 9 Staircase effect for overhanging surface, SEM image and schematics



7 Special defects

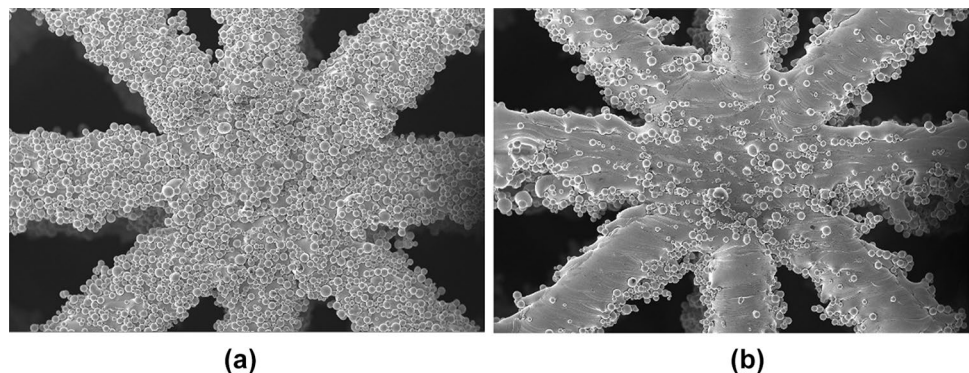
7.1 Issue with build direction

Following the AM thresholds and recommended build-orientation does not guarantee the successful print. Some defects may still exist and need special treatment. As an example, identifying suitable build-orientation may be more problematic for some topologies. Octet-Truss sample#11 was oriented on the build-plate following recommendation of this paper and printed on the corner as indicated in Fig. 16a, b. However, the corner nodes and adjacent struts on the bottom side edge (after orientation) were not printed properly. The defect is less significant for the similar sample #12 in Fig. 16b with thicker struts. Figure 16c indicates one of the defected struts colored by indigo respect to build-plate direction (yellow line). A closer look to this region reveals the need of structural support due to initiating the print on the bed of powder. To resolve the issue, the build orientation is changed by rotating the sample 35° around only one axis and printing this sample on the edge. As it is demonstrated in Fig. 16d, the same strut is now getting printed in an angle. Figure 16e, f indicate that flaw does not exist after this modification, even for larger samples #13 with 5 mm cell size and 0.4-mm strut diameter.

7.2 Issue with thermal distortion

Another common issue is the distortion associated with thermal residual stress. Figure 17a compares an example of cross sections (perpendicular to build-orientation) for strut- and surface-based lattices during the printing process. Pathway for heat dissipation is only thin rods for strut-based lattices, whereas it is thin wide walls for surface-based counterparts. Due to poor heat pathway, locally accumulated heat causes thermal residual stress and distortion. This distortion causes different issues for strut-based lattices including deviation from CAD geometry (yellow arrow in Fig. 17b. In some cases with insufficient heat pathways (support only for one edge in Fig. 17c or small support in Fig. 17d), cracks appeared at the intersection of structural support with the part or build-plate (yellow arrow in Fig. 17c). If the crack propagates suddenly, it changes configuration of the printed portion of the part in the middle of process. This causes a crash with the recoating wiper or line-shift defect as indicated by green line and yellow arrow in Fig. 17d. The solution for this issue is providing a larger heat pathway by placing structural support for the entire length of two supported edges as it is shown in Fig. 17e.

Fig. 10 SEM images of partially melted powder on bounded on bottom (a) and top (b) side of FCC lattice



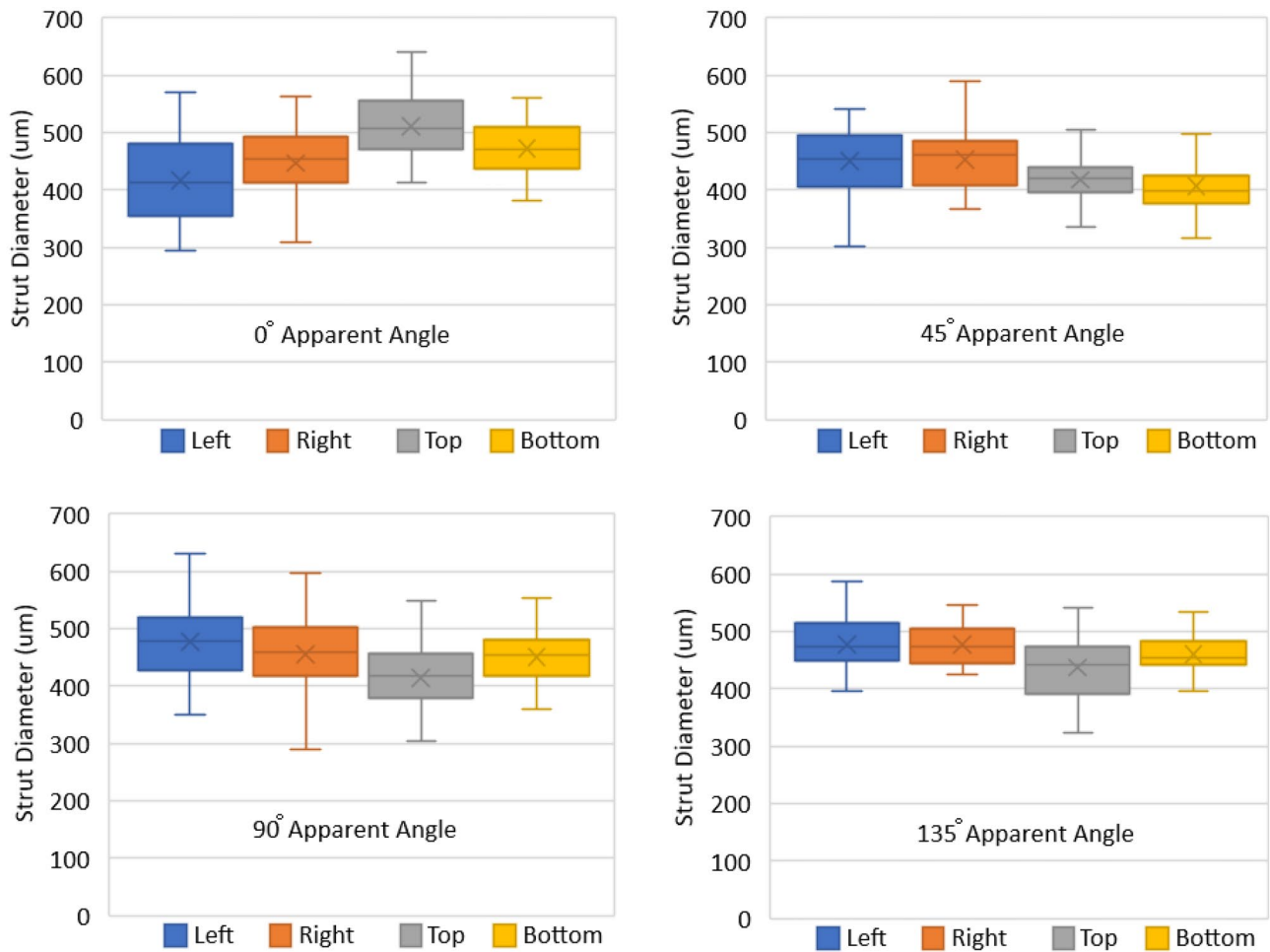


Fig. 11 Strut diameters at different side plans with apparent angle of 0°, 45°, 90°, 135°

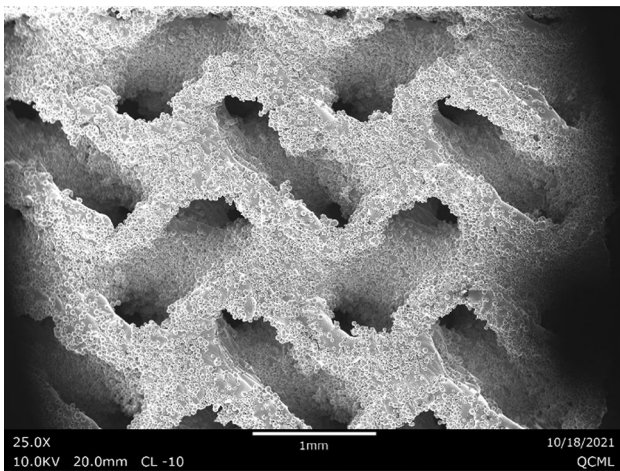


Fig. 12 SEM image of Gyroid ($L = 10 \text{ mm}$, $t = 100 \text{ }\mu\text{m}$)

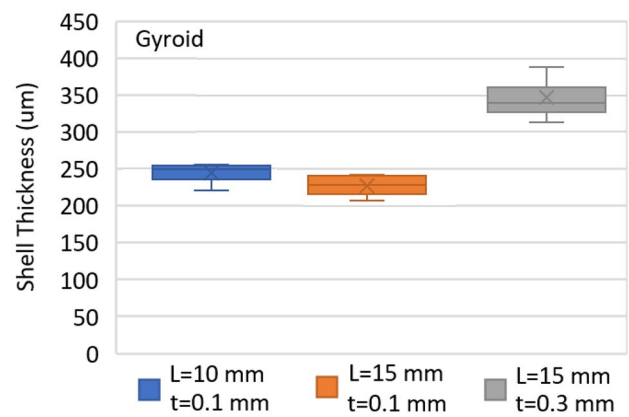


Fig. 13 Gyroid lattices shell thickness

Fig. 14 Samples printed on corner; **a** diagonal #2, **b** FCC #5

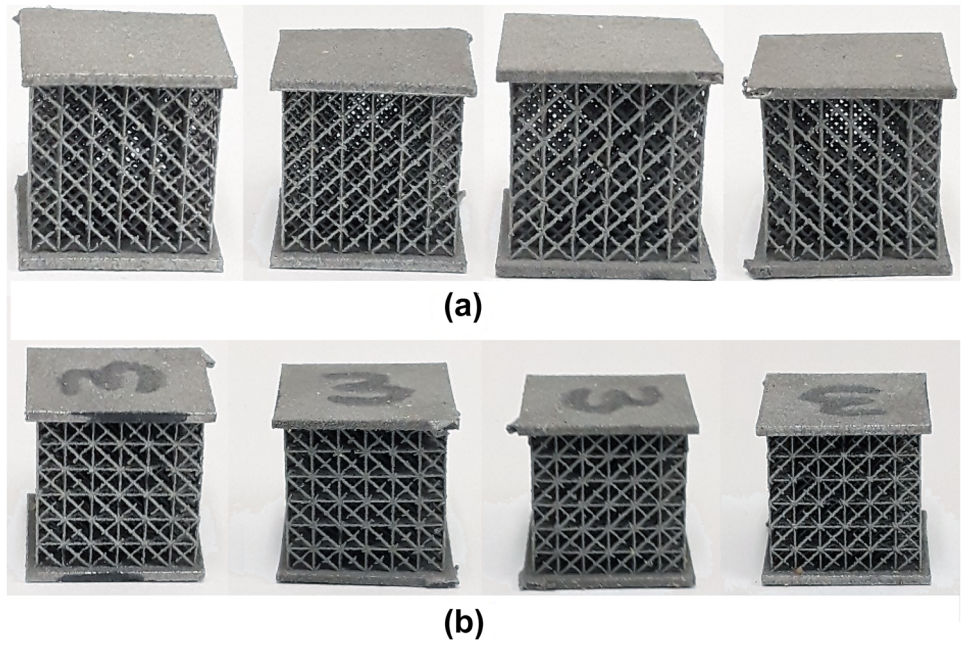


Fig. 15 SEM images of FCC samples with strut length and diameter of **a, b** 1.67 mm and 0.2 mm, **c, d** 2.5 mm and 0.2 mm

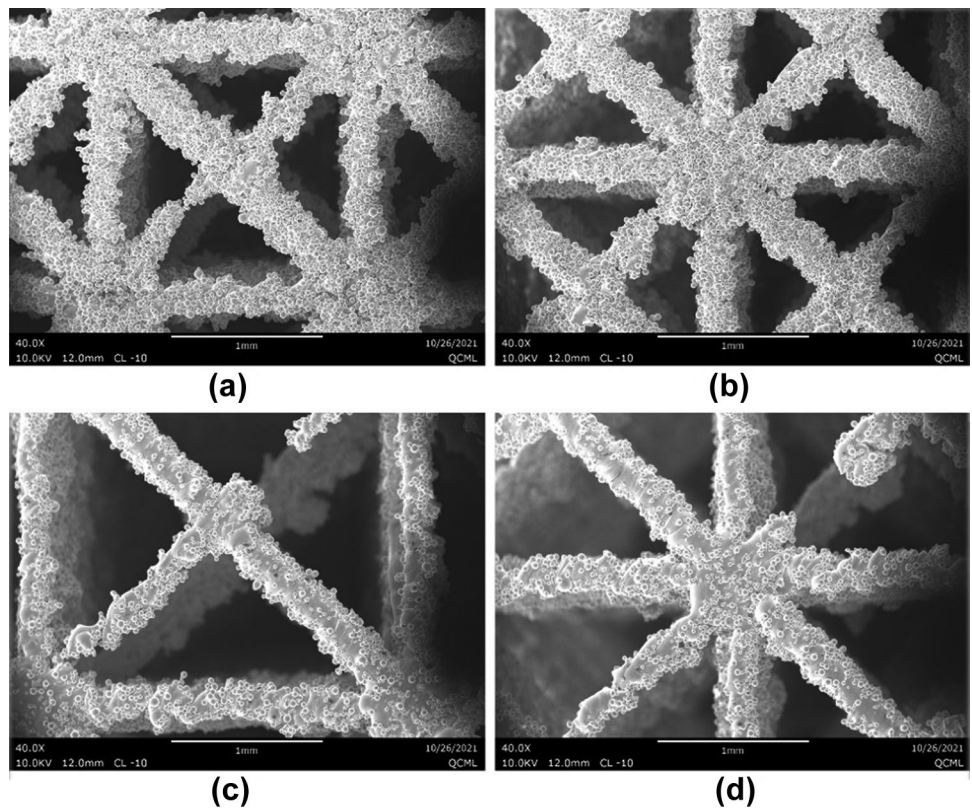


Fig. 16 Octet-Truss samples; **a** severity of flaw for sample #11, **b** sample #12 oriented on build-plate, **c** sample printed on corner, **d** sample printed on edge, **e, f** no flaw for sample #13

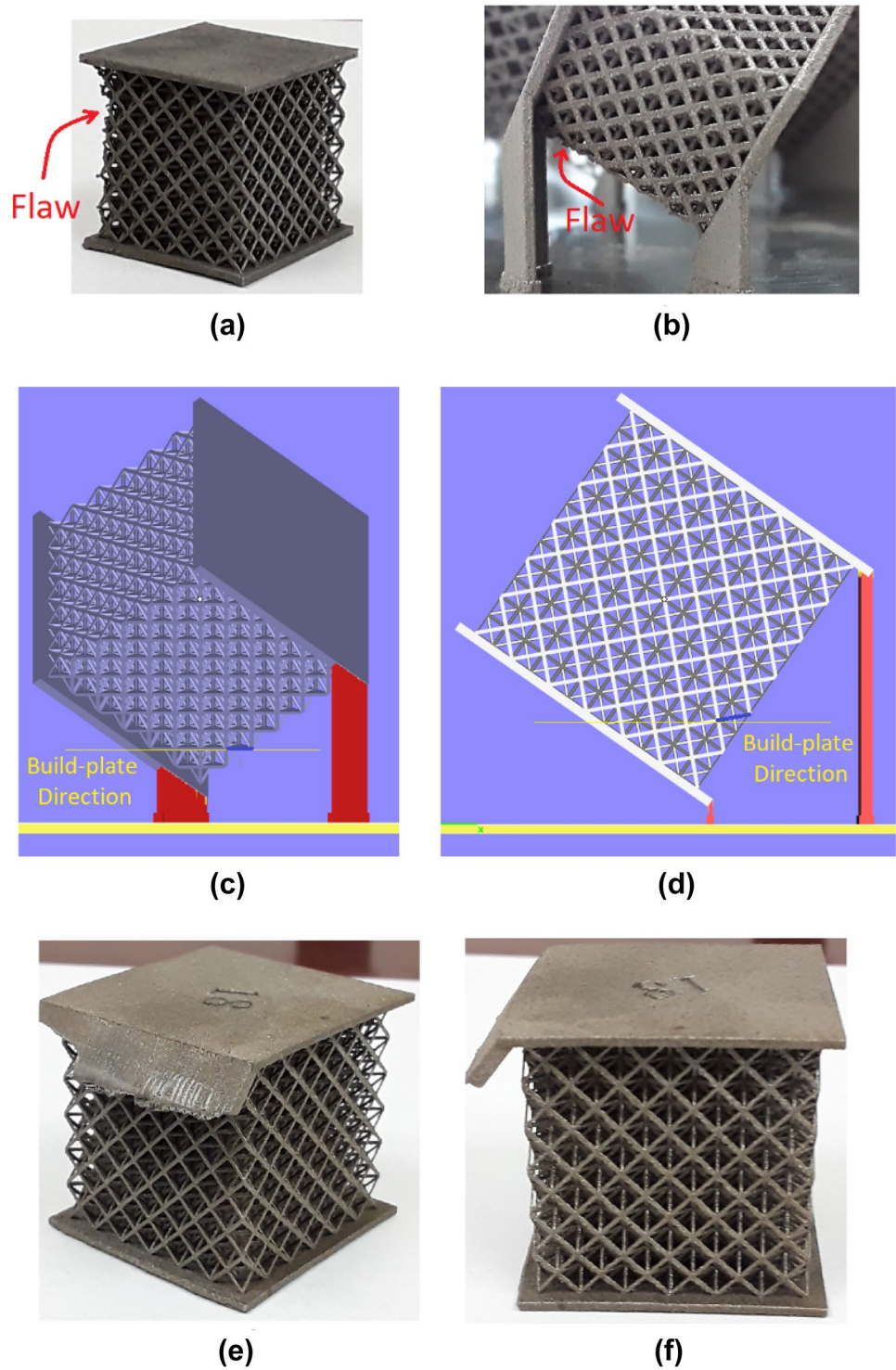
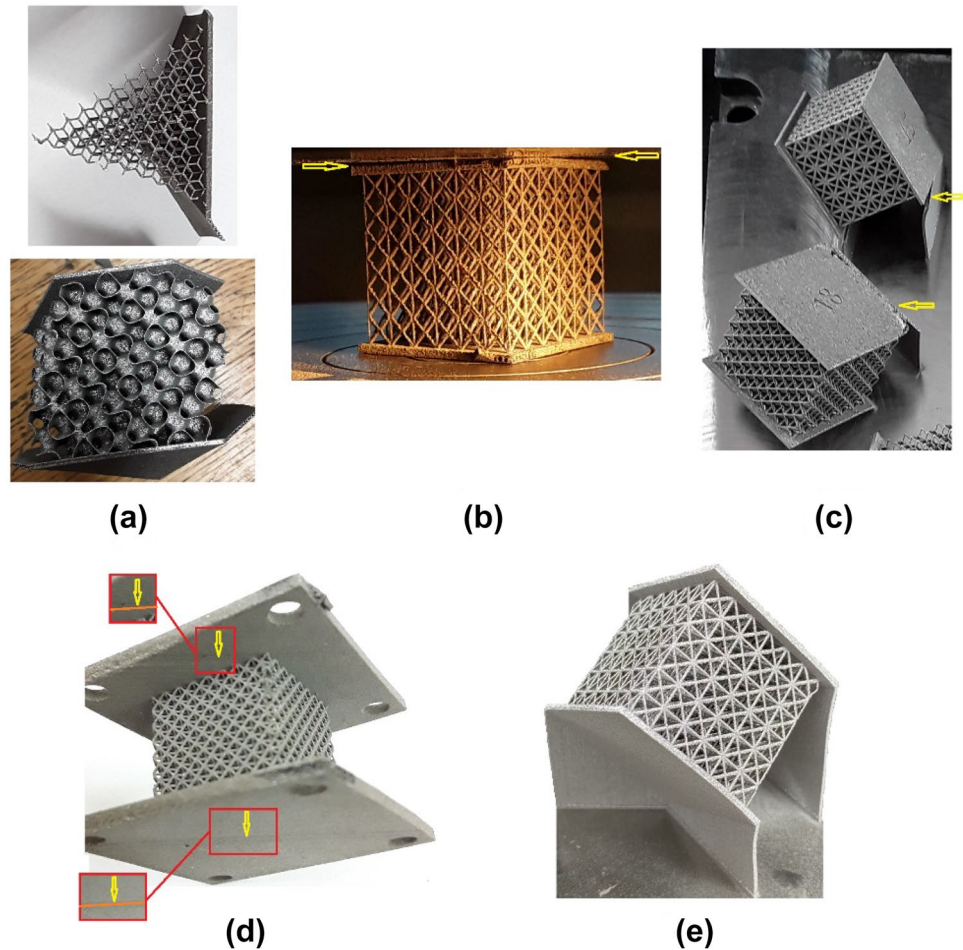


Fig. 17 Issues caused by thermal residual stress, **a** cross-section of strut- and surface-based lattices, **b** distortion, **c** crack, **d** line shift, **e** large support at entire edge



8 Conclusion

Examining lattices at different dimensions improves development of design thresholds because not only it considers the physics of the build process, feedstock, and AM system, but also, it implements the effects of some particular features of printing lattices including structural joints, heat exchange in complex geometry, and variety in build orientation. Investigation on the limits is conducted in this paper with the following outcomes:

- Although delicate components of lattices can be printed without any visible flaw or defect, it is possible that the geometry does not follow the CAD design. Therefore, dimensional accuracy is a criterion to establish thresholds.
- The layer-wise nature of LPBF processes creates effects such as staircase effect and different surface quality for the top and bottom of the part (with respect to build orientation). These inherent features of the process cannot be eliminated.
- Some defects including partially printed struts and excessive powder adhered at surface can be mitigated by changing build process including build orientation.
- The experimental observation demonstrates that partially melted powder particles on the boundary and powder adhesion underneath melt-pool are the main reasons for oversized prints.
- Undesired interaction of laser and powder or recoating wiper and solidified melt-pool may lead to curvature for struts and deviation from CAD design.
- Due to orientation at small angles, struts at top and bottom side are prone to suffer from defects including lack of fusion or curved posture.
- The manufacturability thresholds for printing lattices from Ti-6Al-4V using LPBF process are identified in this paper as 0.4 mm for strut diameter and 0.3 mm for wall thickness.
- Considering the average size of powder particles, the dimensional error is more problematic for delicate parts like thin walls in surface-based lattices or small struts in strut-based lattices.

- Depending on the build-orientation, dimensional accuracy of features varies through the structure even for similar features at different locations. This uneven distribution is less important at dimension above the identified AM thresholds.
- Printing the features with a size below the thresholds leads to significant flaw for strut or highly inaccurate thickness for walls. Significant variation in strut size along the length is observed and geometry is sensitive to real build orientation for the specified feature.
- To avoid heat accumulation and part distortion, the support structure should be enough large to provide a sufficient path for heat dissipation.

Acknowledgements The authors appreciate the funding received from Army Research Lab Cooperative Agreement W911NF-18-2-0067 for enabling this work.

Author contribution All authors contributed to the study conception and design, material preparation, data collection, and analysis.

Funding This work was supported by the funding received from Army Research Lab Cooperative Agreement W911NF-18-2-0067.

Availability of data and material Data and material will be available upon request.

Code availability No code is used in this research.

Declarations

Ethics approval Authors approve to follow the Ethical Responsibilities of Authors for this journal.

Consent to participate All authors read the final manuscript.

Consent for publication All authors approved the publication of the final manuscript.

Competing interests The authors declare no competing interests.

References

1. Tang Y, Dong G, Zhou Q, Zhao YF (2018) Lattice structure design and optimization with additive manufacturing constraints. *IEEE Trans Autom Sci Eng* 15(4):1546–1562
2. Cabanettes F, Joubert A, Chardon G, Dumas V, Rech J, Grosjean C, Dimkovski Z (2018) Topography of as built surfaces generated in metal additive manufacturing: a multi scale analysis from form to roughness. *Precis Eng* 52:249–265
3. Alghamdi A, Downing D, McMillan M, Brandt M, Qian M, Leary M (2019) Experimental and numerical assessment of surface roughness for Ti6Al4V lattice elements in selective laser melting. *Int J Adv Manuf Technol* 105:1275–1293
4. Chahid Y, Racasan R, Pagani L, Townsend A, Liu A, Bills P, Blunt L (2021) *Addit Manuf* 37:101731
5. Lynch ME, Williams K, Cabrera M, Beccuti T (2021) Surface finishing of additively manufactured IN718 lattices by electrochemical machining. *Int J Adv Manuf Technol* 113(4):1–18. <https://doi.org/10.1007/s00170-020-05699-8>
6. Yuan L, Ding S, Wen C (2019) Additive manufacturing technology for porous metal implant applications and triple minimal surface structures: a review. *Bioact Mater* 4:56–70
7. Tancogne-Dejean T, Spierings AB, Mohr D (2016) Additively-manufactured metallic micro-lattice materials for high specific energy absorption under static and dynamic loading. *Acta Mater* 116:14–28
8. Gangireddy S, Faierson EJ, Mishra RS (2018) Influences of post-processing, location, orientation, and induced porosity on the dynamic compression behavior of Ti–6Al–4V alloy built through additive manufacturing. *J Dyn Behav Mater* 4:441–451. <https://doi.org/10.1007/s40870-018-0157-3>
9. Gangireddy S, Komarasamy M, Faierson EJ, Mishra RS (2019) High strain rate mechanical behavior of Ti-6Al-4V octet lattice structures additively manufactured by selective laser melting (SLM). *Mater Sci Eng A* 745:231–239
10. Harris JA, Winter RE, McShane GJ (2017) Impact response of additively manufactured metallic hybrid lattice materials. *Int J Impact Eng* 104:177–191
11. Yan C, Hao L, Hussein A, Raymont D (2012) Evaluations of cellular lattice structures manufactured using selective laser melting. *Int J Mach Tools Manuf* 62:32–38
12. Al-Saedi DSJ, Masood SH, Faizan-Ur-Rab M, Alomarah A, Ponnusamy P (2018) Mechanical properties and energy absorption capability of functionally graded F2BCC lattice fabricated by SLM. *Mater Des* 144:32–44
13. Scalzo F, Totis G, Vaglio E, Sortino M (2021) Experimental study on the high-damping properties of metallic lattice structures obtained from SLM. *Precis Eng* 71:63–77
14. Kang D, Park S, Son Y, Yeon S, Kim SH, Kim I (2019) Multi-lattice inner structures for high-strength and light-weight in metal selective laser melting process. *Mater Des* 175:107786
15. Calignano F (2014) Design optimization of supports for overhanging structures in aluminum and titanium alloys by selective laser melting. *Mater Des* 64:203–213
16. Su XB, Yang YQ, Yu P, Sun JF (2012) Development of porous medical implant scaffolds via laser additive manufacturing. *Trans Nonferrous Metals Soc China* 22(Suppl. 1):181–187
17. Wang X, Xu S, Zhou S, Xu W, Leary M, Choong P, Qian M, Brandt M, Xie YM (2016) Topological design and additive manufacturing of porous metals for bone scaffolds and orthopaedic implants: A review. *Biomaterials* 83:127–141
18. Mazur M, Leary M, Sun S, Vcelka M, Shidid D, Brandt M (2016) Deformation and failure behaviour of Ti-6Al-4V lattice structures manufactured by selective laser melting (SLM). *Int J Adv Manuf Technol* 84:1391–1411

Publisher's Note Springer Nature remains neutral with regard to jurisdictional claims in published maps and institutional affiliations.

Springer Nature or its licensor (e.g. a society or other partner) holds exclusive rights to this article under a publishing agreement with the author(s) or other rightsholder(s); author self-archiving of the accepted manuscript version of this article is solely governed by the terms of such publishing agreement and applicable law.